

Selective Inhibition of Human Solute Carrier Transporters by Multikinase Inhibitors

Rosie A. Johnston, Tristan Rawling, Ting Chan, Fanfan Zhou, and Michael Murray

Pharmacogenomics and Drug Development Group, Discipline of Pharmacology, School of Medical Sciences, Sydney Medical School (R.A.J., M.M.) and Faculty of Pharmacy (T.C., F.Z.), University of Sydney, New South Wales, Australia; and Discipline of Pharmacy, Graduate School of Health, University of Technology, Ultimo, New South Wales, Australia (T.R.)

Received May 14, 2014; accepted August 27, 2014

ABSTRACT

Solute carrier (SLC) transporters regulate the cellular influx and disposition of endogenous and xenobiotic compounds, including anticancer agents such as the multikinase inhibitors (MKIs). Recent evidence suggests that MKIs may also inhibit SLC-dependent transport of coadministered drugs, although present information on the relative susceptibilities of multiple SLC transporters is limited. This study evaluated 18 MKI drugs and metabolites as inhibitors of prototypic substrate uptake by 13 SLC transporters that were overexpressed in human embryonic kidney cells. Organic anion transporting polypeptides (OATPs) 1A2, 1B3, and 2B1, organic

anion transporter 3 (OAT3), and organic cation transporter 1 (OCT1) were inhibited by most MKIs, whereas substrate uptake by OATP1B1, OAT1, 2, and 4, OCT2 and 3, and organic zwitterion/cation transporter 1 (OCTN1) was less susceptible to inhibition; OCTN2 was also inhibited by cediranib. In further studies, IC₅₀ values were determined for the most effective MKIs, and erlotinib and cediranib were found to be potent competitive inhibitors of OATP2B1 (K_i = 41 nM) and OATP1A2 (K_i = 33 nM), respectively. From predictive approaches, several MKI-SLC interactions were found to be of potential *in vivo* significance.

Introduction

Multikinase inhibitor (MKI) drugs target defective signaling pathways that promote the growth and survival of tumor cells. Although MKIs generally produce fewer adverse effects than conventional anticancer drugs, a number have been implicated in toxicities, as well as pharmacokinetic and other interactions that may decrease the safety and efficacy of coadministered drugs (Swaisland et al., 2005; van Erp et al., 2009; Di Gion et al., 2011).

Most pharmacokinetic interactions involving MKIs that have been described to date have focused on biotransformation enzymes and efflux transporters (Liu et al., 2010; Scheffler et al., 2011; Filppula et al., 2012; Gu et al., 2014). However, solute carrier (SLC) transporters are determinants of drug uptake into cells and drug disposition. SLC transporters include organic anion transporting polypeptides (OATPs), organic anion transporters (OATs), organic cation transporters (OCTs), and organic zwitterion/cation transporters (OCTNs). A number of studies have demonstrated that MKIs are important SLC transporter substrates (van Erp et al., 2009; Minematsu and Giacomini, 2011; Hu et al., 2014).

Inhibition of SLC transporters may decrease the efficacy and clearance of coadministered drugs. Several MKIs inhibit the cellular influx of important SLC substrates (Minematsu and Giacomini, 2011;

Karlgren et al., 2012; Hu et al., 2014). At present, however, information on the selectivity of inhibitory interactions across major SLC is not readily available, especially for some of the newer MKIs. The present study assessed the capacity of 18 MKIs to inhibit substrate uptake by 13 OATP, OAT, OCT, and OCTN proteins that were overexpressed in human cells. Predictive estimates of the potential *in vivo* significance of potent inhibitory interactions were also undertaken. The major finding was that the MKIs erlotinib, cediranib, and gefitinib inhibit the activity of specific human influx transporters that could impair the efficacy of coadministered drugs or precipitate pharmacokinetic drug interactions.

Materials and Methods

Chemicals and Biochemicals. Sorafenib and its metabolites (*N'*-hydroxymethylsorafenib *N*-oxide, sorafenib *N*-oxide, *N'*-hydroxymethylsorafenib, *N'*-desmethylsorafenib, and *N'*-desmethylsorafenib *N*-oxide) were synthesized as described previously (Ghassabian et al., 2012). Other MKIs were purchased from Selleck Chemicals (Houston, TX).

[³H]Estrone-3-sulfate (E3S; 57.3 Ci/mmol), [³H]cholecystokinin octapeptide (CCK-8; 97.5 Ci/mmol), and [³H]1-methyl-4-pyridinium acetate (MPP⁺; 82.1 Ci/mmol) were purchased from PerkinElmer (Melbourne, VIC, Australia). [³H]Para-aminohippuric acid (60 Ci/mmol), [³H]L-ergothioneine (1.7 Ci/mmol), and [¹⁴C]L-carnitine (56 mCi/mmol) were purchased from BioScientific Pty. Ltd. (Gynea, NSW, Australia). Unless otherwise stated, cell culture media and all reagents were obtained from Invitrogen (Mount Waverley, VIC, Australia).

Plasmid cDNAs encoding human OATP1A2 (reference sequence: NM_005075.1), OATP1B1 (AB026257.1), OATP1B3 (NM_019844), and OATP2B1 (NM_007256) were obtained from United BioResearch Pty. Ltd. (Dural, NSW, Australia); those

This work was supported by a grant from Cancer Council New South Wales [Grant RG09-14]. R.A.J. was the recipient of a Northcote Graduate Scholarship Award from The Britain-Australia Society.

dx.doi.org/10.1124/dmd.114.059097.

ABBREVIATIONS: CCK-8, cholecystokinin octapeptide; cLogP, calculated logarithm (base 10) of the oil/water partition coefficient; C_{max,u}, maximal unbound MKI concentrations in plasma; C_{max,u(portal)}, maximal unbound concentration of unbound MKI in portal blood at the entrance to the liver; E3S, estrone-3-sulfate; f_u, unbound fraction in plasma; k_a, absorption rate constant; MKI, multikinase inhibitor; MPP⁺, 1-methyl-4-pyridinium acetate; OAT, organic anion transporter; OATP, organic anion transporting polypeptide; OCT, organic cation transporter; OCTN, organic zwitterion/cation transporter; PSA, polar surface area; SLC, solute carrier.

encoding human OAT1 (NM_004790.4), OAT2 (NM_006672.2), OAT3 (NM_004254.2), OCT1 (NM_003057.2), OCT2 (NM_003058.2), and OCT3 (NM_021977.2) were from Australian Biosearch (Balcatta, WA, Australia); and those encoding human OCTN1 (NM_003059) and OCTN2 (NM_003060) were obtained from Gene-Ethics (Asia) Pty. Ltd. (The Franklin, Singapore). Human OAT4 cDNA was obtained as described previously (Zhou et al., 2010).

Transport Studies in Transfected Human Embryonic Kidney 293 Cells. Transporter substrate uptake assays were conducted essentially as described elsewhere (Zhou et al., 2010, 2011). Human embryonic kidney 293 cells (HEK293; American Type Culture Collection, Manassas, VA) were cultured in Dulbecco's modified Eagle's medium supplemented with 10% fetal bovine serum (37°C) and were seeded in 48-well human fibronectin-coated plates (2×10^5 cells/well). Twenty-four hours later, cells were transfected (0.32 μg of plasmid cDNA/well; Lipofectamine 2000; Invitrogen) and substrate uptake assays were conducted after a further 24 hours, as described by Zhou et al. (2011). Protein was estimated by the method of Bradford (1976).

In these experiments, substrate concentrations were as follows: OATP1A2, OATP1B1, OATP2B1, and OAT3 ($[^3\text{H}]$ E3S 300 nM, 68.8 nCi); OATP1B3 ($[^3\text{H}]$ CCK-8 2 nM, 23.4 nCi); OAT1 ($[^3\text{H}]$ para-aminohippuric acid 5 μM , 144 nCi); OAT2 ($[^3\text{H}]$ E3S 2 μM , 138 nCi, pH 5.5); OAT4 ($[^3\text{H}]$ E3S 300 nM, 138 nCi); OCT1, OCT2, and OCT3 ($[^3\text{H}]$ MPP⁺ 100 nM, 98.5 nCi); OCTN1 ($[^3\text{H}]$ L-ergothioneine 5 μM , 40.8 nCi); and OCTN2 ($[^{14}\text{C}]$ L-carnitine 5 μM , 6.72 nCi). MKIs were added to confluent cells in dimethylsulfoxide (0.1% final concentration), and uptake was terminated after 8 minutes by rapidly washing the cells with ice-cold phosphate-buffered saline; substrate uptake was linear under these conditions. The cells were then solubilized in 0.2 M NaOH, neutralized with 0.2 M HCl, and aliquoted for liquid scintillation counting (Ultima Gold scintillation cocktail, Tri-Carb 2810TR; PerkinElmer, Waltham, MA). Uptake was standardized to the amount of protein in each well and corrected for passive permeability by subtraction of the background counts of vector transfected cells. Inhibitor concentrations up to 100 μM did not alter apparent uptake rates. Experiments were performed in triplicate wells on three separate occasions except for those involving OCTs 1–3 and OAT2, which were conducted in duplicate.

Inhibition Studies. MKIs were tested initially at 10 μM . When inhibition exceeded 50%, IC_{50} values were determined (eight concentrations) in triplicate and repeated in three separate experiments. Kinetic studies were undertaken for inhibitory interactions where $\text{IC}_{50} < 0.1 \mu\text{M}$ (OATP2B1- and OATP1A2-mediated uptake of E3S by erlotinib and cediranib, respectively). Michaelis-Menten parameters were determined by nonlinear regression (Prism 6.0; GraphPad Software Inc., La Jolla, CA), and K_i values and mode of inhibition were determined from Lineweaver-Burk and Dixon plots and appropriate replots (Segel, 1975); kinetic experiments were conducted on three occasions.

In Vitro–In Vivo Predictions. The potential in vivo significance of the potent inhibitory interactions that were identified in vitro in transfected HEK293 cells was assessed, as outlined elsewhere (Ito et al., 1998; Giacomini et al., 2010).

Where available, literature data on the maximal plasma concentrations of MKIs (C_{max}) and unbound fraction in plasma (f_u) were used to calculate maximal unbound MKI concentrations in plasma ($C_{\text{max,u}}$). IC_{50} and $C_{\text{max,u}}$ data were then analyzed according to eq. 1. If f_u values for particular MKIs were not available, a conservative estimate was used ($f_u = 0.1$):

$$C_{\text{max,u}}/\text{IC}_{50} \quad (1)$$

$C_{\text{max,u}}/\text{IC}_{50}$ values ≥ 0.1 indicated that the IC_{50} was less than 10-fold the unbound maximal systemic concentration of MKI in plasma ($C_{\text{max,sys}}$) in cells expressing OAT or OCT proteins; these interactions were analyzed further. The maximal unbound concentration of unbound MKI in portal blood at the entrance to the liver [$C_{\text{max,u(portal)}}$] was calculated using the following equation (Ito et al., 1998; Giacomini et al., 2010):

$$C_{\text{max,u(portal)}} = C_{\text{max,u}} + \frac{(f_u/r_B) \cdot \text{Dose} \cdot F_a \cdot k_a}{Q_h} \quad (2)$$

where f_u is the unbound fraction of the MKI in plasma, r_B is the blood-to-plasma concentration ratio, Dose is the maximum oral dose of the MKI, F_a is the reported oral bioavailability of the MKI, k_a is the absorption rate constant, and Q_h is hepatic blood flow rate (1.61 l/min; Ito et al., 1998). Two values of k_a were evaluated: 0.1/min, which is the theoretical maximal value considering

gastric emptying rate (Ito et al., 1998), and 0.03/min, as suggested by Giacomini et al. (2010).

R values were then calculated as follows:

$$R = 1 + \frac{f_u \cdot C_{\text{max,portal}}}{\text{IC}_{50}} \quad (3)$$

$$\text{or, } R = 1 + \frac{f_u \cdot C_{\text{max,portal}}}{K_i} \quad (4)$$

Physicochemical Properties. The structures of the test MKIs are shown in Fig. 1. Physicochemical parameters for MKIs were determined [molecular weight, the logarithm (base 10) of the oil/water partition coefficient calculated by the fragment approach (cLogP), total polar surface area (PSA), number of rotatable bonds, hydrogen bond-donor groups and hydrogen bond-acceptor groups (ChemBioDraw Ultra 13.0; PerkinElmer)] and used in linear and multiple regression analysis to evaluate relationships between IC_{50} values for inhibition of SLC-mediated substrate uptake.

Data Analysis and Statistics. Initial inhibition data were analyzed by one-way analysis of variance, and Bonferroni's multiple comparison test was used to detect differences from control (Prism 6.0). IC_{50} and Michaelis-Menten kinetic parameters were determined by nonlinear regression.

Results and Discussion

Eighteen MKIs were tested for the capacity to modulate substrate uptake by 13 SLC transporters expressed in HEK293 cells (Fig. 1). Initial screening at the 10 μM concentration identified a number of potent inhibitory interactions (>50% inhibition); IC_{50} values were determined for these interactions (Table 1). Ten MKIs exhibited IC_{50} values in the range 0.03–3.77 μM for the inhibition of E3S uptake by OATP1A2, with only lapatinib, bosutinib, and sorafenib and its metabolites exhibiting <50% inhibition when tested at the 10 μM concentration. OATP2B1-mediated E3S uptake was also inhibited by gefitinib, nilotinib, afatinib, erlotinib, pelitinib, and neratinib (IC_{50} values 0.03–2.68 μM). In contrast, OATP1B3-mediated CCK-8 uptake was only effectively inhibited by neratinib and erlotinib, whereas IC_{50} values were determined for inhibition of MPP⁺ uptake by OCT1 and L-carnitine uptake by OCTN2 by bosutinib and cediranib, respectively (Table 1). In contrast, substrate uptake by OATP1B1; OATs 1, 2, and 4; OCTs 2 and 3; and OCTN1 was less readily inhibited by the present group of MKIs.

Two particularly potent interactions were identified—inhibition of OATP2B1-mediated E3S uptake by erlotinib and inhibition of OATP1A2-mediated E3S uptake by cediranib (IC_{50} values 0.03 μM). Kinetic constants were determined for E3S uptake by OATP2B1 (K_m $3.4 \pm 0.8 \mu\text{M}$ and V_{max} $21.3 \pm 2.1 \text{ pmol/min per } \mu\text{g protein}$; Fig. 2A); previous studies in transfected HEK293 and Caco-2 cells reported similar K_m values for E3S uptake of 8.1 and 1.6 μM , respectively (Nozawa et al., 2004; Sai et al., 2006). Inhibition of E3S transport by erlotinib exhibited a K_i of 41 nM (Fig. 2, B and C). Dixon and Dixon slope replot analyses were consistent with competitive inhibition (Fig. 2, D and E; Segel, 1975). In the case of E3S uptake by OATP1A2, the K_m was $9.0 \pm 1.1 \mu\text{M}$ and V_{max} was $52.8 \pm 2.6 \text{ pmol/min per } \mu\text{g protein}$ (Fig. 3A); cediranib was found to be a competitive inhibitor of E3S uptake by OATP1A2 (K_i 33 nM; Fig. 3). Previous studies in transfected HEK293 and Chinese hamster ovary cells reported similar K_m values for E3S uptake by OATP1A2 of 12.5 and 2.4 μM , respectively (Cui et al., 2001; Gui et al., 2008).

Predictive approaches were used to assess the potential in vivo significance of potent in vitro inhibitory interactions. In these approaches, values for the unbound drug concentrations in plasma and IC_{50} data were analyzed using eq. 1. It has been proposed that the criterion $C_{\text{max,u}}/\text{IC}_{50} \geq 0.1$ (i.e., that the unbound peak serum

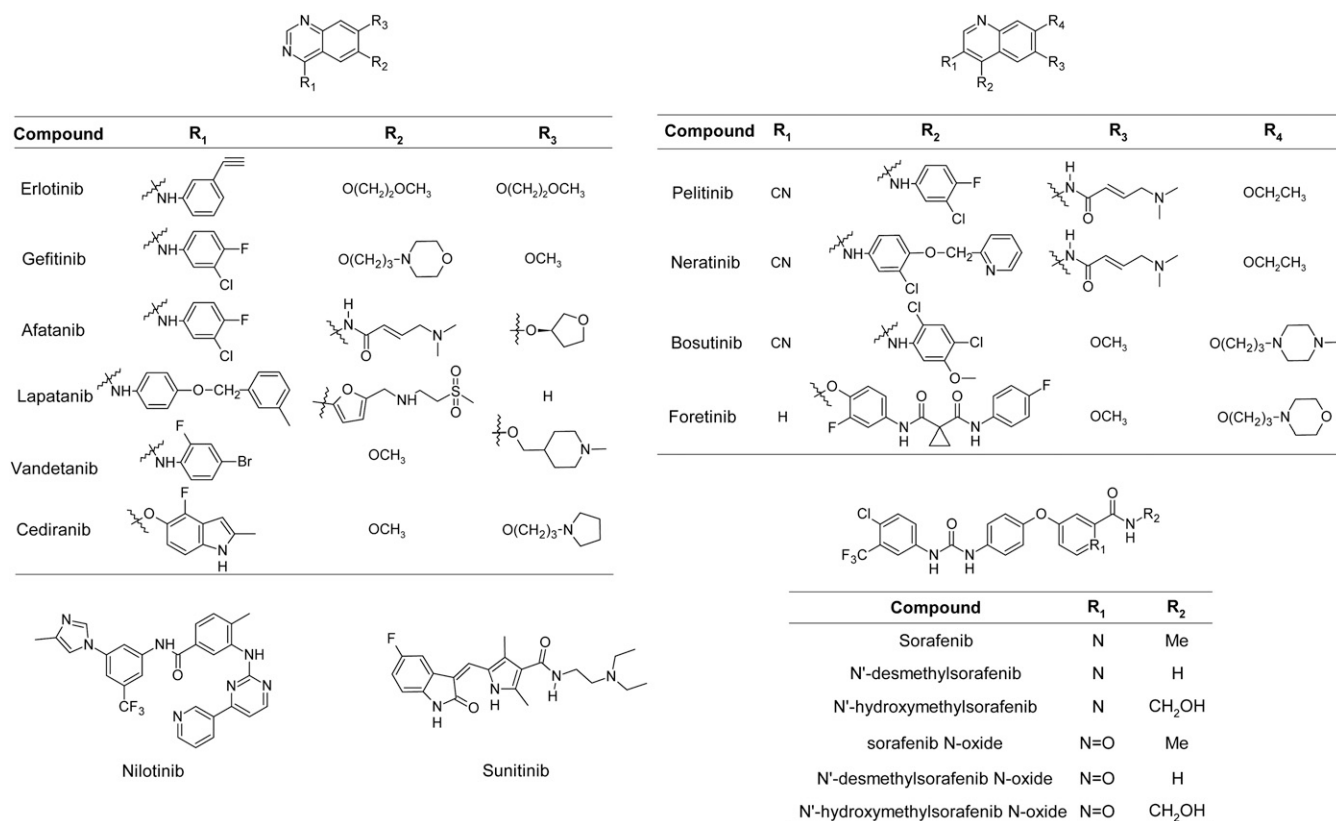


Fig. 1. Structures of MKIs used in this study.

concentration is at least one-tenth of that required for 50% inhibition *in vitro*) should be met for potential clinical significance (Ito et al., 1998; Giacomini et al., 2010). As shown in Table 2, inhibition of OATP1A2, OATP1B3, and, in particular, OATP2B1 by erlotinib;

inhibition of OATP1A2 by cediranib; inhibition of OATP2B1 by gefitinib; and inhibition of OAT3 by nilotinib met this criterion. In further analyses, the unbound steady-state concentration of these MKIs in portal blood was calculated (eq. 2). In these calculations, two

 TABLE 1
 Inhibition of SLC transporter-dependent substrate uptake by MKI drugs

Data are presented as IC₅₀ values or means ± S.D. of three individual reactions expressed as percentage of control (solvent alone).

MKI	SLC Transporter ^d						
	OATP1A2 (E3S) ^b	OATP1B1 (E3S)	OATP1B3 (CCK-8)	OATP2B1 (E3S)	OAT3 (E3S)	OCT1 (MPP ⁺)	OCTN2 (L-Carnitine)
Gefitinib	0.88	105 ± 3	78 ± 3	0.65	66 ± 5***	57 ± 5***	92 ± 4
Lapatinib	72 ± 2***	123 ± 13	98 ± 16	84 ± 0.5**	85 ± 7	96 ± 9	99 ± 8
Nilotinib	1.45	110 ± 7	100 ± 3	2.67	0.41	91 ± 1	99 ± 2
Sunitinib	2.03	109 ± 10	101 ± 10	88 ± 1	67 ± 3***	67 ± 7***	81 ± 6
Bosutinib	55 ± 3***	121 ± 6	109 ± 5	111 ± 3	81 ± 11	2.06	86 ± 10
Vandetanib	2.45	110 ± 6	71 ± 5***	82 ± 5***	75 ± 2**	68 ± 1***	106 ± 6
Afatinib	1.17	119 ± 4	66 ± 3***	2.08	97 ± 0.4	80 ± 8***	98 ± 3
Cediranib	0.03	103 ± 5	64 ± 5***	79 ± 3***	73 ± 10**	54 ± 2***	2.49
Erlotinib	1.10	104 ± 5	1.19	0.03	81 ± 2	86 ± 4*	92 ± 3
Pelitinib	3.77	104 ± 4	66 ± 1***	2.01	82 ± 0.4	76 ± 1***	94 ± 5
Neratinib	0.39	110 ± 10	0.65	2.68	73 ± 2**	77 ± 2***	92 ± 4
Foretinib	3.55	96 ± 7	68 ± 0.5***	54 ± 0.5***	63 ± 8***	74 ± 4***	91 ± 4
Sorafenib	90 ± 11	114 ± 0.1	109 ± 4	79 ± 1***	90 ± 11	99 ± 0.4	94 ± 8
N'-Hydroxymethylsorafenib N-oxide	64 ± 9**	64 ± 9***	66 ± 4***	70 ± 1***	51 ± 5***	93 ± 0.4	89 ± 1
Sorafenib N-oxide	78 ± 6***	81 ± 1***	80 ± 3	66 ± 5***	79 ± 1	108 ± 2	87 ± 4
N'-Hydroxymethylsorafenib	85 ± 6	101 ± 4	113 ± 8	90 ± 4	73 ± 12**	103 ± 5	96 ± 4
N'-Desmethylsorafenib	101 ± 5	59 ± 1***	130 ± 9	103 ± 5	81 ± 7	111 ± 0.4	108 ± 0.4
N'-Desmethylsorafenib N-oxide	91 ± 8	108 ± 2	96 ± 4	99 ± 8	61 ± 6***	109 ± 3	116 ± 4

^aFold increases in substrate uptake in SLC cDNA-transfected to untransfected cells (mean ± S.E.M., n = 3–8) were as follows: OATP1A2 (16.0 ± 0.01), OATP1B1 (23.5 ± 2), OATP1B3 (7.4 ± 0.7), OATP2B1 (5.0 ± 0.5), OAT1 (10.6 ± 0.2), OAT2 (1.9 ± 0.01), OAT3 (30.0 ± 1.2), OAT4 (7.6 ± 0.02), OCT1 (11.3 ± 0.05), OCT2 (10.0 ± 0.4), OCT3 (16.8 ± 0.04), OCTN1 (23.9 ± 0.2), and OCTN2 (20.8 ± 0.03).

^bTransporter substrate.

Inhibition relative to control: *P < 0.05, **P < 0.01, ***P < 0.001.

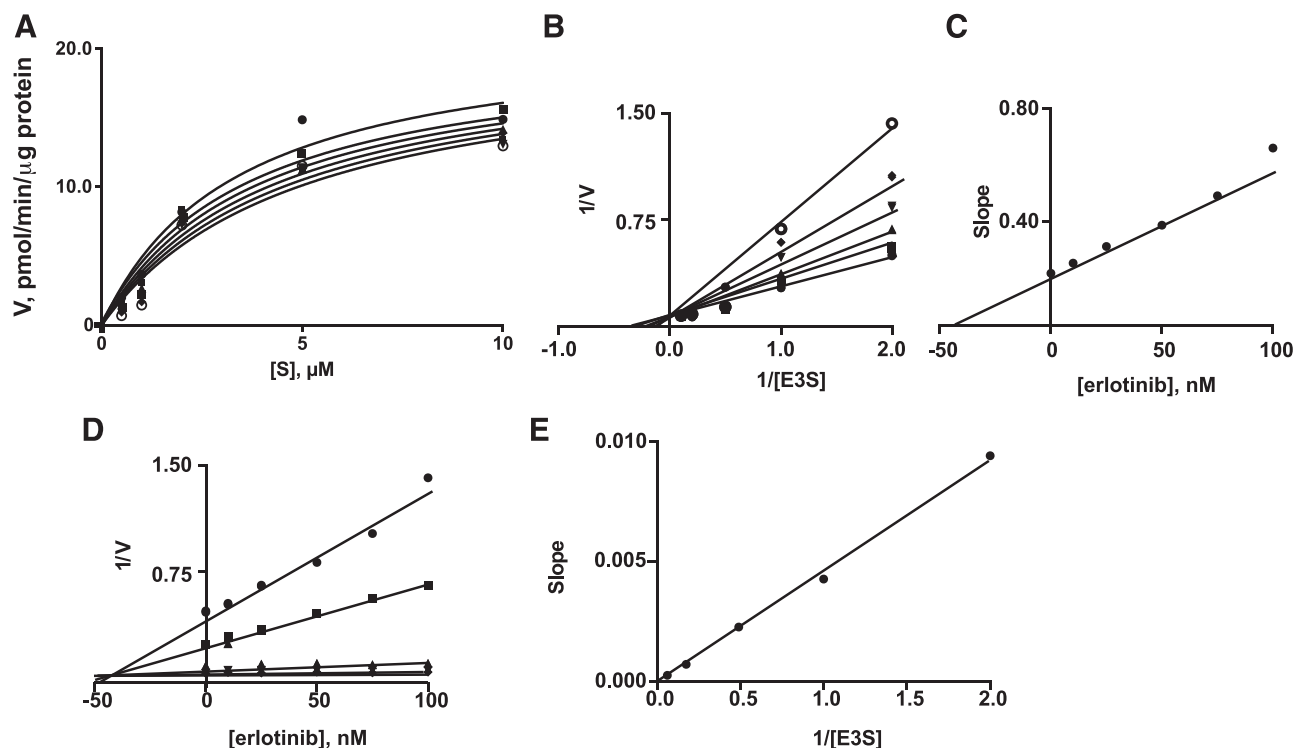


Fig. 2. Inhibition by erlotinib of OATP2B1-mediated E3S uptake in transfected HEK293 cells. (A) Michaelis-Menten plots of E3S uptake in the presence of different concentrations of erlotinib: (●) 0 nM, (■) 10 nM, (▲) 25 nM, (▼) 50 nM, (◆) 75 nM, and (○) 100 nM. (B) Lineweaver-Burk plots of the data. (C) Replot of the slopes from the Lineweaver-Burk plots. (D) Dixon plots in the presence of different concentrations of E3S: (●) 0.5 μ M, (■) 1 μ M, (▲) 2 μ M, (▼) 5 μ M, and (◆) 10 μ M. (E) Replot of the slopes from the Dixon plots. Units of E3S uptake (V): pmol/min per μ g protein. A representative analysis from three individual experiments is shown; kinetic constants varied by less than 8%.

values for the absorption rate constant (k_a) were tested, 0.03 and 0.1, which represent conservative and apparent maximal rates of intestinal absorption, respectively. IC_{50} values and, where determined, K_i values

were then analyzed by eq. 3 and 4 to determine R values that reflect the predicted increase in drug exposure from the available MKI entering the liver; the criterion $R > 2.0$ is taken as the cutoff and

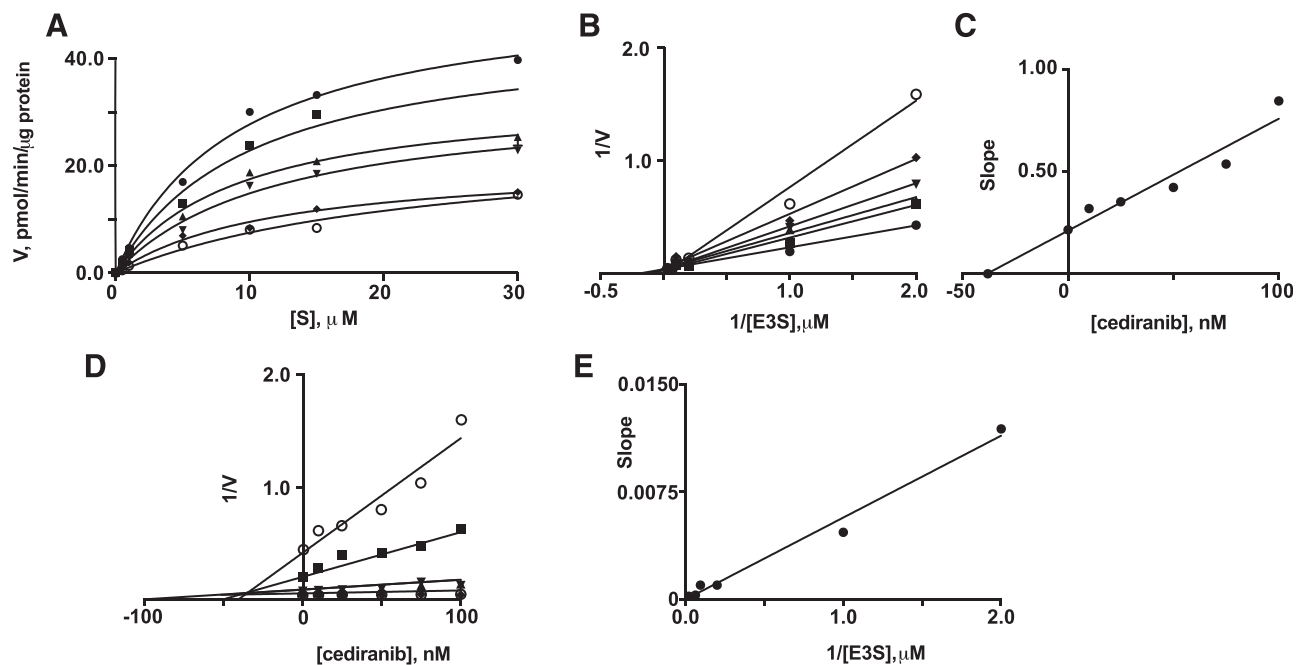


Fig. 3. Inhibition by cediranib of OATP1A2-mediated E3S uptake in transfected HEK293 cells. (A) Michaelis-Menten plots of E3S uptake in the presence of different concentrations of cediranib: (●) 0 nM, (■) 10 nM, (▲) 25 nM, (▼) 50 nM, (◆) 75 nM, and (○) 100 nM. (B) Lineweaver-Burk plots of the data. (C) Replot of the slopes from the Lineweaver-Burk plots. (D) Dixon plots in the presence of different concentrations of E3S: (○) 0.5 μ M, (■) 1 μ M, (▼) 5 μ M, (▲) 10 μ M, (◆) 15 μ M, and (●) 30 μ M. (E) Replot of the slopes from the Dixon plots. Units of E3S uptake (V): pmol/min per μ g protein. A representative analysis from three individual experiments is shown; kinetic constants varied by less than 8%.

TABLE 2

In vitro IC₅₀ values for inhibition of SLC transporter-mediated substrate uptake by MKIs and in vivo unbound plasma concentrations (C_{max,u})

MKI	IC ₅₀	C _{max,u} ^a	C _{max,u} /IC ₅₀	References
<i>μM</i>				
OATP1A2				
Afatinib	1.17	0.009	0.01	http://www.accessdata.fda.gov/drugsatfda_docs/label/2013/201292s002lbl.pdf ; Wind et al., 2013
Cediranib	0.03	0.006	0.20	Yamamoto et al., 2009; McTigue et al., 2012
Erlotinib	1.10	0.322	0.29	Yamamoto et al., 2008; van Erp et al., 2009
Foretanib ^b	3.55	0.016 ^c	0.004 ^c	Naing et al., 2012
Gefitinib	0.88	0.090	0.10	Nakagawa et al., 2003; van Erp et al., 2009
Neratinib ^b	0.39	0.013 ^c	0.03 ^c	Wong et al., 2009
Nilotinib	1.46	0.085	0.06	Hazarika et al., 2008; Tanaka et al., 2010; Larson et al., 2012
Pelitinib ^b	3.77	0.008 ^c	0.02 ^c	Erlichman et al., 2006
Sunitinib	2.03	0.007	0.003	van Erp et al., 2009; Shirao et al., 2010
Vandetanib	2.45	0.037	0.02	Mross et al., 2009
OATP1B3				
Erlotinib	1.19	0.322	0.27	Yamamoto et al., 2008; van Erp et al., 2009
Neratinib ^b	0.65	0.013 ^c	0.02 ^c	Wong et al., 2009
OATP2B1				
Afatinib	2.08	0.009	0.004	http://www.accessdata.fda.gov/drugsatfda_docs/label/2013/201292s002lbl.pdf ; Wind et al., 2013
Erlotinib	0.03	0.322	10.7	Yamamoto et al., 2008; van Erp et al., 2009
Gefitinib	0.65	0.090	0.14	Nakagawa et al., 2003; van Erp et al., 2009
Neratinib ^b	2.68	0.013 ^c	0.01 ^c	Wong et al., 2009
Nilotinib	2.67	0.085	0.03	Hazarika et al., 2008; Tanaka et al., 2010
Pelitinib ^b	2.01	0.008 ^c	0.004 ^c	Erlichman et al., 2006
OAT3				
Nilotinib	0.41	0.051	0.13	Hazarika et al., 2008; Tanaka et al., 2010
OCT1				
Bosutinib	2.06	0.016	0.01	http://www.accessdata.fda.gov/drugsatfda_docs/label/2013/203341s001lbl.pdf ; Hsyu et al., 2013
OCTN2				
Cediranib	2.49	0.006	0.002	Yamamoto et al., 2009; McTigue et al., 2012

^aCalculated as C_{max} × f_u.

^bInformation on C_{max,u} unavailable.

^cA conservative estimate of f_u = 0.1, consistent with a number of other MKIs was used in these calculations.

predicts a 2-fold increase in drug exposure (Ito et al., 1998; Giacomini et al., 2010). Thus, the inhibition of OATP2B1-dependent uptake by erlotinib could have great potential significance (R = 16.1–45.0; Table 3). Inhibition of OATP1A2 by cediranib and inhibition of OATP2B1 by gefitinib may also be significant (R = 2.00–5.43), but R values for the other interactions only exceeded the criterion at the higher k_a value (Table 3).

The present findings suggest that there is potential for interaction between erlotinib or gefitinib and substrates of OATP2B1, which

include drugs such as montelukast, aliskiren, and certain statins, and endogenous molecules, such as sulfated estrogens, thyroxine, and taurocholate (Noé et al., 2007; Roth et al., 2012). Similarly, erlotinib and cediranib may elicit interactions with OATP1A2 substrates that include the anticancer agents imatinib, methotrexate, and hydroxyurea (Hu et al., 2008; Walker et al., 2011; Roth et al., 2012). Erlotinib may also precipitate interactions with OATP1B3 that also transports drugs, such as the anticancer agents docetaxel, hydroxyurea, imatinib, methotrexate, and paclitaxel (Smith et al., 2005; Walker et al., 2011; Roth et al., 2012).

TABLE 3

Parameters used to calculate C_{max,u(portal)} and R values for MKIs with C_{max,u}/IC₅₀ > 0.1

Data were obtained from the following references: Frohna et al., 2006; Hazarika et al., 2008; Hughes et al., 2009; van Erp et al., 2009; Yamamoto et al., 2009; Tanaka et al., 2010; Larson et al., 2012; McTigue et al., 2012; O'Brien and Fallah Moghaddam, 2013.

MKI	Dose	F _a	f _u	C _{max,u(portal)}		R[k _a 0.03] ^a	R[k _a 0.1]	R[k _a 0.03]	R[k _a 0.1]
				k _a 0.03	k _a 0.1	eq. 3	eq. 3	eq. 4	eq. 4
<i>mg</i>									
<i>μM</i>									
OATP1A2									
Cediranib	30	1	0.03	0.037	0.130	2.23	5.43	2.12	4.94
Erlotinib	150	0.60	0.07	0.620	1.32	1.56	2.20		
OATP1B3									
Erlotinib						1.52	2.11		
OATP2B1									
Erlotinib						21.7	45.0	16.1	33.2
Gefitinib	250	0.59	0.09	0.818	2.52	2.26	4.88		
OAT3									
Nilotinib	300	0.31	0.02	0.117	0.270	1.29	1.66		

F_a, reported oral bioavailability of the MKI.

^af_B = 1, except for gefitinib (0.76; Li et al., 2006).

TABLE 4
Physicochemical properties of MKIs

Data calculated using ChemBioDraw Ultra 13.0 Suite (PerkinElmer).

MKI	Molecular Weight	cLogP	PSA	Rotatable Bonds	H-Bond Donors	H-Bond Acceptors
Sorafenib	464.8	5.46	91.8	5	3	7
Gefitinib	446.9	5.45	67.7	7	1	7
Bosutinib	530.5	4.94	82.4	9	1	8
Erlotinib	393.4	4.19	73.7	9	1	7
Lapatinib	581.1	6.05	101.4	10	2	8
Vandetanib	475.4	5.69	58.5	5	1	6
Pelitinib	467.9	5.14	89.8	8	2	7
Nilotinib	529.5	5.69	93.8	7	2	8
Afatinib	485.9	4.34	87.6	7	2	8
Neratinib	557.1	5.00	111.3	11	2	9
Sunitinib	398.5	3.00	73.5	7	3	6
Cediranib	450.5	5.28	67.7	8	1	7
Foretanib	632.7	5.57	110.7	12	2	10
<i>N'</i> -Desmethylsorafenib	450.8	5.14	105.8	5	4	7
Sorafenib <i>N</i> -oxide	480.1	3.34	114.2	5	3	8
<i>N'</i> -Desmethylsorafenib <i>N</i> -oxide	466.8	3.08	128.2	5	4	8
<i>N'</i> -Hydroxymethylsorafenib	480.1	4.92	112.1	7	4	8
<i>N'</i> -Hydroxymethylsorafenib <i>N</i> -oxide	496.8	2.81	134.4	7	4	9

The MKIs tested belong to four heterocyclic classes. As shown in Fig. 1, six are substituted quinazolines, four are quinolone derivatives, nilotinib and the sorafenib analogs are substituted pyridines, and sunitinib is an indolinone. The three most effective transporter inhibitors, erlotinib, gefitinib, and cediranib, are substituted quinazolines, suggesting that this structural moiety mediates potent inhibition. However, other members of the class—afatinib, lapatinib, and vandetanib—were not especially potent inhibitors. Attempts to define a structure activity relationship using common medicinal chemistry descriptors such as cLogP, number of rotatable bonds/H-bond acceptors/H-bond donors, and PSA were inconclusive. Erlotinib, gefitinib, and cediranib all had relatively small PSAs, seven to eight rotatable bonds, seven H-bond acceptors, and only one H-bond donor (Table 4). In contrast, the inactive quinazolines lapatinib and afatinib had larger PSAs that may contribute to decreased permeability and two H-bond donor atoms; both vandetanib and lapatinib had high cLogP values. Previous studies have shown that lipophilic character is negatively correlated with inhibition of some SLC transporters (Minematsu and Giacomini, 2011) but is a determinant of substrate interactions with OATs and OATPs (Chang et al., 2005; Kaler et al., 2007; De Bruyn et al., 2013).

At present, there is a limited amount of information regarding the capacity of MKI drugs to interact with human influx transporters. Several of the drugs have been found to be substrates or inhibitors of organic cation transporters (Minematsu and Giacomini, 2011; Roth et al., 2012) and organic anion transporters (Roth et al., 2012; Hu et al., 2014). The present findings that erlotinib is a potent inhibitor of E3S uptake by OATP2B1, whereas OATP1B1 and OATP1B3 are less responsive to the drug, are consistent with an earlier report (Karlgrén et al., 2012). However, the interactions of MKIs with SLC transporters may also be influenced by the particular substrate used in assays (Izumi et al., 2013) and by the duration of incubations (Shitara et al., 2013). In the present study, CCK-8 uptake by OATP1B3 was inhibited by erlotinib with an IC_{50} of 1.19 μ M, whereas the IC_{50} for inhibition of estradiol 17β -glucuronide uptake was higher at 44 μ M (Karlgrén et al., 2012). Similarly, two studies conducted in different cell types reported apparently conflicting findings that sorafenib was (Zimmerman et al., 2013) and was not (Hu et al., 2009) transported by OATP1B1. These authors suggested that cell context may affect xenobiotic transport. In this regard, it was reported recently that sorafenib was a potent inhibitor of docetaxel transport in OATP1B1-transfected

Flp-In-T-Rex293 cells after a 15-minute preincubation ($IC_{50} \sim 0.07 \mu$ M; Hu et al., 2014), whereas E3S uptake by OATP1B1 in HEK293 cells (without preincubation) was only weakly inhibited in the present study by two sorafenib metabolites.

MKI-SLC transporter interactions could impair drug clearance if the transporter has a major exclusive role in elimination, but it is also very likely that impaired uptake into target cells could diminish efficacy. Unlike pharmacokinetic interactions, which are readily identified by altered drug concentrations in serum and may produce toxicity, decreased uptake into cells is more difficult to detect since this compartment cannot be sampled conveniently. However, such interactions may lead to failure of therapy, and further studies, including uptake studies in cancer cell lines and pharmacokinetic interaction studies in vivo, are now required to directly test the clinical significance of the MKI-SLC interactions detected in the present study.

Authorship Contributions

Participated in research design: Johnston, Zhou, Murray.
Conducted experiments: Johnston, Rawling, Chan, Zhou.
Contributed new reagents or analytic tools: Rawling.
Performed data analysis: Johnston, Chan, Zhou, Murray.
Wrote or contributed to the writing of the manuscript: Johnston, Rawling, Zhou, Murray.

References

- Bradford MM (1976) A rapid and sensitive method for the quantitation of microgram quantities of protein utilizing the principle of protein-dye binding. *Anal Biochem* **72**:248–254.
- Chang C, Pang KS, Swaan PW, and Ekins S (2005) Comparative pharmacophore modeling of organic anion transporting polypeptides: a meta-analysis of rat Oatp1a1 and human OATP1B1. *J Pharmacol Exp Ther* **314**:533–541.
- Cui Y, König J, Leier I, Buchholz U, and Keppler D (2001) Hepatic uptake of bilirubin and its conjugates by the human organic anion transporter SLC21A6. *J Biol Chem* **276**:9626–9630.
- De Bruyn T, van Westen GJ, Ijzerman AP, Stieger B, de Witte P, Augustijns PF, and Annaert PP (2013) Structure-based identification of OATP1B1/3 inhibitors. *Mol Pharmacol* **83**:1257–1267.
- Di Gion P, Kanefendt F, Lindauer A, Scheffler M, Doroshenko O, Fuhr U, Wolf J, and Jaehde U (2011) Clinical pharmacokinetics of tyrosine kinase inhibitors: focus on pyrimidines, pyridines and pyrroles. *Clin Pharmacokinet* **50**:551–603.
- Erllichman C, Hidalgo M, Boni JP, Martins P, Quinn SE, Zacharchuk C, Amorusi P, Adjei AA, and Rowinsky EK (2006) Phase I study of EKB-569, an irreversible inhibitor of the epidermal growth factor receptor, in patients with advanced solid tumors. *J Clin Oncol* **24**:2252–2260.
- Filippula AM, Laitila J, Neuvonen PJ, and Backman JT (2012) Potent mechanism-based inhibition of CYP3A4 by imatinib explains its liability to interact with CYP3A4 substrates. *Br J Pharmacol* **165**:2787–2798.
- Frohna P, Lu J, Eppler S, Hamilton M, Wolf J, Rakhit A, Ling J, Kenkare-Mitra SR, and Lum BL (2006) Evaluation of the absolute oral bioavailability and bioequivalence of erlotinib, an inhibitor of the epidermal growth factor receptor tyrosine kinase, in a randomized, crossover study in healthy subjects. *J Clin Pharmacol* **46**:282–290.

- Ghassabian S, Rawling T, Zhou F, Doddareddy MR, Tattam BN, Hibbs DE, Edwards RJ, Cui PH, and Murray M (2012) Role of human CYP3A4 in the biotransformation of sorafenib to its major oxidized metabolites. *Biochem Pharmacol* **84**:215–223.
- Giacomini KM, Huang SM, Tweedie DJ, Benet LZ, Brouwer KL, Chu X, Dahlin A, Evers R, Fischer V, and Hillgren KM, et al.; International Transporter Consortium (2010) Membrane transporters in drug development. *Nat Rev Drug Discov* **9**:215–236.
- Gu R, Hibbs DE, Ong JA, Edwards RJ, and Murray M (2014) The multikinase inhibitor axitinib is a potent inhibitor of human CYP1A2. *Biochem Pharmacol* **88**:245–252.
- Gui C, Miao Y, Thompson L, Wahlgren B, Mock M, Stieger B, and Hagenbuch B (2008) Effect of pregnane X receptor ligands on transport mediated by human OATP1B1 and OATP1B3. *Eur J Pharmacol* **584**:57–65.
- Hazarika M, Jiang X, Liu Q, Lee SL, Ramchandani R, Garnett C, Orr MS, Sridhara R, Booth B, and Leighton JK, et al. (2008) Tasigna for chronic and accelerated phase Philadelphia chromosome—positive chronic myelogenous leukemia resistant to or intolerant of imatinib. *Clin Cancer Res* **14**:5325–5331.
- Hsyu PH, Mould DR, Upton RN, and Amantea M (2013) Pharmacokinetic-pharmacodynamic relationship of bosutinib in patients with chronic phase chronic myeloid leukemia. *Cancer Chemother Pharmacol* **71**:209–218.
- Hu S, Chen Z, Franke R, Orwick S, Zhao M, Rudek MA, Sparreboom A, and Baker SD (2009) Interaction of the multikinase inhibitors sorafenib and sunitinib with solute carriers and ATP-binding cassette transporters. *Clin Cancer Res* **15**:6062–6069.
- Hu S, Franke RM, Filipki KK, Hu C, Orwick SJ, de Bruijn EA, Burger H, Baker SD, and Sparreboom A (2008) Interaction of imatinib with human organic ion carriers. *Clin Cancer Res* **14**:3141–3148.
- Hu S, Mathijssen RH, de Bruijn P, Baker SD, and Sparreboom A (2014) Inhibition of OATP1B1 by tyrosine kinase inhibitors: in vitro-in vivo correlations. *Br J Cancer* **110**:894–898.
- Hughes AN, O'Brien ME, Petty WJ, Chick JB, Rankin E, Woll PJ, Dunlop D, Nicolson M, Boimpally R, and Wolf J, et al. (2009) Overcoming CYP1A1/1A2 mediated induction of metabolism by escalating erlotinib dose in current smokers. *J Clin Oncol* **27**:1220–1226.
- Ito K, Iwatsubo T, Kanamitsu S, Ueda K, Suzuki H, and Sugiyama Y (1998) Prediction of pharmacokinetic alterations caused by drug-drug interactions: metabolic interaction in the liver. *Pharmacol Rev* **50**:387–412.
- Izumi S, Nozaki Y, Komori T, Maeda K, Takenaka O, Kusano K, Yoshimura T, Kusuura H, and Sugiyama Y (2013) Substrate-dependent inhibition of organic anion transporting polypeptide 1B1: comparative analysis with prototypical probe substrates estradiol-17 β -glucuronide, estrone-3-sulfate, and sulfobromophthalein. *Drug Metab Dispos* **41**:1859–1866.
- Kaler G, Truong DM, Khandelwal A, Nagle M, Eraly SA, Swaan PW, and Nigam SK (2007) Structural variation governs substrate specificity for organic anion transporter (OAT) homologs. Potential remote sensing by OAT family members. *J Biol Chem* **282**:23841–23853.
- Karlgrén M, Vildhede A, Norinder U, Wisniewski JR, Kimoto E, Lai Y, Haglund U, and Artursson P (2012) Classification of inhibitors of hepatic organic anion transporting polypeptides (OATPs): influence of protein expression on drug-drug interactions. *J Med Chem* **55**:4740–4763.
- Larson RA, Yin OQ, Hochhaus A, Saglio G, Clark RE, Nakamae H, Gallagher NJ, Demirhan E, Hughes TP, and Kantarjian HM, et al. (2012) Population pharmacokinetic and exposure-response analysis of nilotinib in patients with newly diagnosed Ph+ chronic myeloid leukemia in chronic phase. *Eur J Clin Pharmacol* **68**:723–733.
- Li J, Brahmer J, Messersmith W, Hidalgo M, and Baker SD (2006) Binding of gefitinib, an inhibitor of epidermal growth factor receptor-tyrosine kinase, to plasma proteins and blood cells: in vitro and in cancer patients. *Invest New Drugs* **24**:291–297.
- Liu Y, Ramírez J, House L, and Ratain MJ (2010) Comparison of the drug-drug interactions potential of erlotinib and gefitinib via inhibition of UDP-glucuronosyltransferases. *Drug Metab Dispos* **38**:32–39.
- McTigue M, Murray BW, Chen JH, Deng YL, Solowiej J, and Kania RS (2012) Molecular conformations, interactions, and properties associated with drug efficiency and clinical performance among VEGFR TK inhibitors. *Proc Natl Acad Sci USA* **109**:18281–18289.
- Minematsu T and Giacomini KM (2011) Interactions of tyrosine kinase inhibitors with organic cation transporters and multidrug and toxic compound extrusion proteins. *Mol Cancer Ther* **10**:531–539.
- Mross K, Fasol U, Frost A, Benkelmann R, Kuhlmann J, Büchert M, Unger C, Blum H, Hennig J, and Milenkova TP, et al. (2009) DCE-MRI assessment of the effect of vandetanib on tumor vasculature in patients with advanced colorectal cancer and liver metastases: a randomized phase I study. *J Angiogenesis Res* **1**:5.
- Naing A, Kurzrock R, Adams LM, Kleha JF, Laubscher KH, Bonate PL, Weller S, Fitzgerald C, Xu Y, and LoRusso PM (2012) A comparison of the pharmacokinetics of the anticancer MET inhibitor foretinib free base tablet formulation to bisphosphate salt capsule formulation in patients with solid tumors. *Invest New Drugs* **30**:327–334.
- Nakagawa K, Tamura T, Negoro S, Kudoh S, Yamamoto N, Yamamoto N, Takeda K, Swaisland H, Nakatani I, and Hirose M, et al. (2003) Phase I pharmacokinetic trial of the selective oral epidermal growth factor receptor tyrosine kinase inhibitor gefitinib ('Iressa', ZD1839) in Japanese patients with solid malignant tumors. *Ann Oncol* **14**:922–930.
- Noé J, Portmann R, Brun ME, and Funk C (2007) Substrate-dependent drug-drug interactions between gemfibrozil, fluvastatin and other organic anion-transporting peptide (OATP) substrates on OATP1B1, OATP2B1, and OATP1B3. *Drug Metab Dispos* **35**:1308–1314.
- Nozawa T, Imai K, Nezu J, Tsuji A, and Tamai I (2004) Functional characterization of pH-sensitive organic anion transporting polypeptide OATP-B in human. *J Pharmacol Exp Ther* **308**:438–445.
- O'Brien Z and Fallah Moghaddam M (2013) Small molecule kinase inhibitors approved by the FDA from 2000 to 2011: a systematic review of preclinical ADME data. *Expert Opin Drug Metab Toxicol* **9**:1597–1612.
- Roth M, Obaidat A, and Hagenbuch B (2012) OATPs, OATs and OCTs: the organic anion and cation transporters of the SLCO and SLC22A gene superfamilies. *Br J Pharmacol* **165**:1260–1287.
- Sai Y, Kaneko Y, Ito S, Mitsuoka K, Kato Y, Tamai I, Artursson P, and Tsuji A (2006) Predominant contribution of organic anion transporting polypeptide OATP-B (OATP2B1) to apical uptake of estrone-3-sulfate by human intestinal Caco-2 cells. *Drug Metab Dispos* **34**:1423–1431.
- Scheffler M, Di Gion P, Doroshenko O, Wolf J, and Fuhr U (2011) Clinical pharmacokinetics of tyrosine kinase inhibitors: focus on 4-anilinoquinazolines. *Clin Pharmacokinet* **50**:371–403.
- Segel IH (1975) *Enzyme Kinetics: Behaviour and Analysis of Rapid Equilibrium and Steady-State Enzyme Systems*, John Wiley & Sons, New York.
- Shirao K, Nishida T, Doi T, Komatsu Y, Muro K, Li Y, Ueda E, and Ohtsu A (2010) Phase I/II study of sunitinib malate in Japanese patients with gastrointestinal stromal tumor after failure of prior treatment with imatinib mesylate. *Invest New Drugs* **28**:866–875.
- Shitara Y, Takeuchi K, and Horie T (2013) Long-lasting inhibitory effects of saquinavir and ritonavir on OATP1B1-mediated uptake. *J Pharm Sci* **102**:3427–3435.
- Smith NF, Acharya MR, Desai N, Figg WD, and Sparreboom A (2005) Identification of OATP1B3 as a high-affinity hepatocellular transporter of paclitaxel. *Cancer Biol Ther* **4**:815–818.
- Swaisland HC, Ranson M, Smith RP, Leadbetter J, Laight A, McKillop D, and Wild MJ (2005) Pharmacokinetic drug interactions of gefitinib with rifampicin, itraconazole and metoprolol. *Clin Pharmacokinet* **44**:1067–1081.
- Tanaka C, Yin OQ, Sethuraman V, Smith T, Wang X, Grouss K, Kantarjian H, Giles F, Ottmann OG, and Galitz L, et al. (2010) Clinical pharmacokinetics of the BCR-ABL tyrosine kinase inhibitor nilotinib. *Clin Pharmacol Ther* **87**:197–203.
- van Erp NP, Gelderblom H, and Guchelaar HJ (2009) Clinical pharmacokinetics of tyrosine kinase inhibitors. *Cancer Treat Rev* **35**:692–706.
- Walker AL, Franke RM, Sparreboom A, and Ware RE (2011) Transcellular movement of hydroxyurea is mediated by specific solute carrier transporters. *Exp Hematol* **39**:446–456.
- Wind S, Schmid M, Erhardt J, Goeldner RG, and Stopfer P (2013) Pharmacokinetics of afatinib, a selective irreversible ErbB family blocker, in patients with advanced solid tumours. *Clin Pharmacokinet* **52**:1101–1109.
- Wong KK, Fracaso PM, Bukowski RM, Lynch TJ, Munster PN, Shapiro GI, Jänne PA, Eder JP, Naughton MJ, and Ellis MJ, et al. (2009) A phase I study with neratinib (HKI-272), an irreversible pan ErbB receptor tyrosine kinase inhibitor, in patients with solid tumors. *Clin Cancer Res* **15**:2552–2558.
- Yamamoto N, Horiike A, Fujisaka Y, Murakami H, Shimoyama T, Yamada Y, and Tamura T (2008) Phase I dose-finding and pharmacokinetic study of the oral epidermal growth factor receptor tyrosine kinase inhibitor Ro50-8231 (erlotinib) in Japanese patients with solid tumors. *Cancer Chemother Pharmacol* **61**:489–496.
- Yamamoto N, Tamura T, Yamamoto N, Yamada K, Yamada Y, Nokihara H, Fujiwara Y, Takahashi T, Murakami H, and Boku N, et al. (2009) Phase I, dose escalation and pharmacokinetic study of cediranib (RECENTIN), a highly potent and selective VEGFR signaling inhibitor, in Japanese patients with advanced solid tumors. *Cancer Chemother Pharmacol* **64**:1165–1172.
- Zhou F, Lee AC, Krafczyk K, Zhu L, and Murray M (2011) Protein kinase C regulates the internalization and function of the human organic anion transporting polypeptide 1A2. *Br J Pharmacol* **162**:1380–1388.
- Zhou F, Zhu L, Cui PH, Church WB, and Murray M (2010) Functional characterization of nonsynonymous single nucleotide polymorphisms in the human organic anion transporter 4 (hOAT4). *Br J Pharmacol* **159**:419–427.
- Zimmerman EI, Hu S, Roberts JL, Gibson AA, Orwick SJ, Li L, Sparreboom A, and Baker SD (2013) Contribution of OATP1B1 and OATP1B3 to the disposition of sorafenib and sorafenib-glucuronide. *Clin Cancer Res* **19**:1458–1466.

Address correspondence to: Dr. Michael Murray, Pharmacogenomics and Drug Development Group, Discipline of Pharmacology, School of Medical Sciences, Sydney Medical School, University of Sydney, NSW 2006, Australia. E-mail: michael.murray@sydney.edu.au